Planar Sensors for RFID Wireless Complex-Dielectric-Permittivity Sensing of Liquids

Humberto Lobato-Morales, Alonso Corona-Chávez, José L. Olvera-Cervantes

Instituto Nacional de Astrofísica, Óptica y Electrónica, INAOE, Puebla, Mexico

Abstract — Two planar sensors for wireless RFID dielectric permittivity sensing of liquids are presented. The first sensor consists of a Substrate-Integrated-Waveguide (SIW) resonant cavity while the second one is composed by an SIW Epsilon-Near-Zero (ENZ) tunnel sensor. Both structures produce a notch resonance response at 4 GHz which is used for the characterization of the liquids using the Cavity-Perturbation-Technique. The proposed sensors present good sensitivity using a small amount of sample volume.

Index Terms — dielectric permittivity measurements, Radio Frequency Identification, Substrate-Integrated-Waveguide, Cavity Perturbation Technique, Epsilon-Near-Zero Tunnel.

I. Introduction

The measurement of complex dielectric permittivity of materials is required for several applications including medical, pharmaceutical, industrial, food, experimental, among others [1]. Resonant techniques using cavities have been used for this purpose due to the high sensitivity and high Q factors that can be obtained; moreover, with the development of the Substrate-Integrated-Waveguide (SIW) technology, some planar sensors with good sensitivity and small dimensions have been proposed [2], [3]. In [2], the introduction of SIW resonant cavities is applied for the measurement of complex dielectric permittivity of solvent liquids and binary mixtures. In [3], an SIW Epsilon-Near-Zero (ENZ) sensor for complex dielectric permittivity of materials is reported presenting smaller dimensions and higher sensitivity compared with SIW cavities

More recently, with the development of chipless Radio-Frequency-Identification (RFID) tags, several applications, going from the scan, detect and identification of objects, have been proposed. Last advances in microwave sensors have provided the capability to merge sensing techniques with RFID systems, expanding its applications to biomedical, industrial and material wireless sensing and monitoring [4]. Basically, an RFID system provides wireless data capturing where the interrogator is used to scan and indentify tagged objects based on the information from the RFID tag located on the object [4]. An RFID tag with a notch spiral resonator loaded with resistive and capacitive sensors for wireless measurements is proposed in [4].

In this paper, two sensors for chipless RFID tags, operating at 4 GHz, are presented for the measurement of complex dielectric permittivity of liquids.

The first sensor (*sensor-A*) consists of an SIW cavity in its TE_{101} mode fed by microstrip lines; the second one (*sensor-B*) is composed by an SIW ENZ tunnel fed by microstrip lines. The Cavity-Perturbation-Technique for SIW structures (SIW-CPT) is applied to characterize the liquid samples. Several liquids are measured and characterized with good agreement with reported values.

With the addition of cross-polarized antennas at their terminals, the proposed sensors can be employed as RFID sensor tags for wireless material sensing and monitoring.

II. Design of Substrate-Integrated-Waveguide sensors

A Substrate-Integrated-Waveguide (SIW) resonant cavity and SIW Epsilon-Near-Zero (ENZ) tunnel are the basic sensors for each of the proposed structures, *sensor-A* and *sensor-B* respectively. Both circuits are implemented on a Rogers RO4003C laminate with relative dielectric permittivity $\varepsilon_r = 3.55$ and height $h = 0.813$ mm, and operate at 4 GHz.

The proposed structures can be used as wireless dielectric-permittivity sensors in an RFID chipless tag configuration with the addition of two antennas (input and output ports) in each of the circuits, as shown in Fig. 1. In such a system, the tag is interrogated by the reader by sending a frequency sweep signal. The Rx tag antenna propagates the signal towards the sensing circuit, which introduces a "transmission zero" with a specific resonant frequency and Q factor depending on the tested material. The processed signal is transmitted back to the reader using the Tx tag antenna. The reader and tag Rx and Tx antennas are cross-polarized in order to minimize interference between the interrogation and retransmitted processed signals [4]. On the tag, the sensors are symmetrically fed in common-mode configuration to produce an optimal de-coupling of the signal producing the "transmission zero", which is easily read in such systems [4] and can be further analyzed using the SIW-CPT.

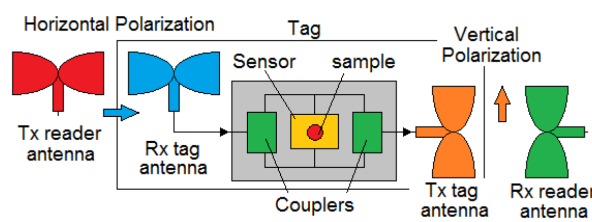

Fig. 1. Chipless RFID permittivity sensor system block diagram.

A. Cavity Sensor (sensor-A)

The SIW cavity is designed in its TE_{101} resonant mode by using [2]

978-1-4673-2141-9/13/$31.00 ©2013 IEEE

$$f_{101} = \frac{c}{2\sqrt{\varepsilon_r}} \sqrt{\left(\frac{1}{a}\right)^2 + \left(\frac{1}{d}\right)^2}\,, \qquad (1)$$

where f_{101} is the resonant frequency, c is the speed of light in a vacuum, a and d are the width and length of the SIW cavity, respectively. From (1), the initial cavity dimensions are $a = d$ = 28 mm, and it is closed by lateral walls of 0.6 mm-diameter metallic posts separated 0.6 mm each other.

Conventional hybrid couplers [5] are used to feed the cavity. An extra transmission line section at one output of the hybrids is added to compensate 90° phase shift at 4 GHz generating a common-mode signal. From simulations [6] the ±5° phase bandwidth of this configuration is greater than 12%, enough for the measurements, as will be shown below. Fig. 2(a) shows the geometry and final dimensions of *sensor-A*.

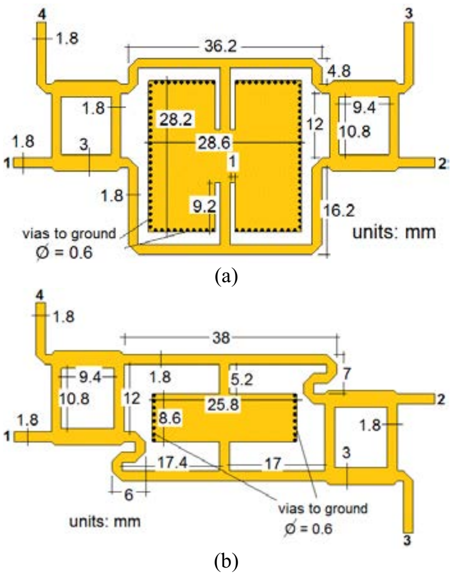

Fig. 2. Geometry and dimensions of (a) *sensor-A*, (b) *sensor-B*.

B. Epsilon-Near-Zero Tunnel Sensor (sensor-B)

The ENZ tunneling effect can be obtained by coupling a narrow-height waveguide in its TE_{10} propagation mode. Although the coupling is originally made using different height waveguides to produce squeezing of the energy along the tunnel [3], it is possible to obtain such an effect by using transmission lines as coupling elements. The tunneling frequency f_t of an SIW ENZ structure is calculated from the cutoff frequency of a TE_{10} propagation mode waveguide [3]

$$f_{c10} = \frac{c}{2b\sqrt{\varepsilon_r}} = f_t\,, \qquad (2)$$

where b corresponds to the width of the SIW. The tunnel length is independent on the width and operating frequency. At f_t a very high and constant electric field is generated inside the SIW along its length, producing the ENZ effect. Initial width of the tunnel operating at 4 GHz is b = 20 mm. A tunnel length l_t = 9mm is proposed. The reader is encouraged to refer [3] for more details in ENZ tunnel design and operation.

In simulations [6], the structure is optimized and connected to hybrid couplers for a common-mode operation the same way as in *sensor-A*. The lateral walls of the tunnel are formed by metallic posts of 0.6 mm diameter spaced 0.6 mm between them. The geometry and final dimensions of *sensor-B* are shown in Fig. 2(b).

C. Sample Position

Although both sensors operate under different mechanisms (resonant cavity and tunneling structure), due to their configuration, the maximum electric field $\bar{\boldsymbol{E}}$ occurs at the center of the SIW cavity and tunnel. A quartz capillary tube with outer and inner diameters of 2.5 mm and 1.5 mm, respectively, is placed perpendicularly to the plane of each sensor through its center; thus, the Liquid-Under-Test (LUT) is interacting with the maximum $\bar{\boldsymbol{E}}$-field producing variations in the frequency responses. With an LUT volume of only 1.44 mm^3 it is possible for the sensors to generate the necessary frequency variations. Fig. 3 shows the simulated [7] response of both structures and their electric field distribution $\bar{\boldsymbol{E}}$.

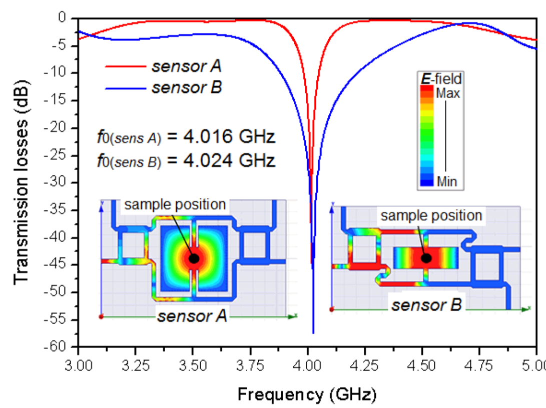

Fig. 3. *Sensors-A* and *-B* simulated frequency response and $\bar{\boldsymbol{E}}$-field distribution at f_0.

III. Liquids-Under-Test Characterization

Both sensors are fabricated and connected to an Agilent *E8361A* Vector-Network-Analyzer, at ports 1 and 2. Ports 3 and 4 are 50 Ω loaded in both circuits.

The Liquids-Under-Test (LUT) are: (*1*) *ethanol*, (*2*) *methanol*, (*3*) *isobutanol*, (*4*) *isopropyl alcohol*, (*5*) *acetonitrile* and (*6*) *deionized water*. The frequency response for each of the LUT is analyzed in terms of resonant frequency and unloaded Q factor by the use of the Cavity-Perturbation-Technique (CPT) for SIW [3]

$$\varepsilon'_s = \frac{A\varepsilon'_r V_c}{V_s}\left(\frac{f_0 - f_s}{f_s}\right) + \varepsilon'_r\,, \qquad (3.a)$$

$$\varepsilon''_s = \frac{BV_c}{V_s}\left(\frac{\varepsilon'^2_r + \varepsilon''^2_r}{\varepsilon'_r}\right)\left(\frac{Q_0 - Q_s}{Q_0 Q_s}\right) + \frac{\varepsilon'_s\,\varepsilon''_r}{\varepsilon'_r}\,, \qquad (3.b)$$

where ε' and ε'' correspond to real and imaginary parts of the complex dielectric permittivity; the subscripts s and r indicate

978-1-4673-2141-9/13/$31.00 ©2013 IEEE

whether sample or substrate permittivity, respectively, is being used; f_0 and f_s, as well as Q_0 and Q_s, are the operating frequencies and unloaded quality factors before the perturbation and after the perturbation with the LUT, respectively; V_c is volume of the cavity and V_s volume of the sample; A and B are constants related with the configuration of the circuits, mode of operation, shape and position of the sample inside the sensors. As the calculation difficulty of A and B is high, they are obtained experimentally by using standard samples of well known dielectric properties [1]-[3].

At room temperature, each of the LUT is measured five times using both sensors, and their f_s and Q averaged for the analysis. The standard samples for A and B calculation are (*1*) *ethanol* and (*2*) *methanol*, whose permittivity values are taken from [8]; A and B are calculated for LUT (*1*) and (*2*) and averaged. Calculations for LUT unloaded Q (Q_s) are from [5]

$$\frac{1}{Q_T}=\frac{1}{Q_{et}}+\frac{1}{Q_s}, \tag{4}$$

where Q_T is the measured Q of the sensor with the LUT and Q_{et} is the measured Q factor of the sensor with an empty tube, assuming that the medium for this case (air) has $\varepsilon'' = 0$.

Table I shows the LUT characterization using *sensor-A* and Table II tabulates the obtained results using *sensor-B*; along with the characterized data are the reported values of liquids (*1*) and (*2*) at 4 GHz (rep) taken from [8].

TABLE I
SENSOR-A LUT CHARACTERIZATION ($A = 3.087$, $B = 2.3428$).

LUT	f_s (GHz)	Q_s	ε'	ε''	ε' (rep)	ε'' (rep)
1	4.030	560.64	5.27	5.51	5.22	3.56
2	4.022	326.66	13.84	9.68	13.99	13.1
3	4.025	1155.46	10.62	2.51	-	-
4	4.032	581.74	3.13	5.29	-	-
5	4.014	894.86	22.44	3.33	-	-
6	4.000	198.32	37.57	16.15	-	-

TABLE II
SENSOR-B LUT CHARACTERIZATION ($A = 9.9835$, $B = 11.2662$).

LUT	f_s (GHz)	Q_s	ε'	ε''	ε' (rep)	ε'' (rep)
1	4.105	628.11	4.84	4.20	5.22	3.56
2	4.094	312.15	15.43	11.36	13.99	13.1
3	4.098	514.68	11.57	5.76	-	-
4	4.106	974.41	3.88	1.69	-	-
5	4.086	925.93	23.17	1.93	-	-
6	4.073	254.75	35.81	14.57	-	-

IV. RESULTS DISCUSSION

Because the proposed sensors are based on different operating principles (cavity and tunnel), their characteristics can be discussed based on their performance. Fig. 4 plots the sensitivity of both sensors for the real and imaginary parts of the LUT permittivity, based on Tables I and II. Photographs of the sensors with their overall dimensions are also shown.

As can be seen in Fig. 4, *sensor-A* presents slightly lower sensitivity for sample ε' than *sensor-B*: 0.92 MHz/$\Delta\varepsilon'$ and 1.03 MHz/$\Delta\varepsilon'$, respectively, where $\Delta\varepsilon'$ is increment in LUT ε' of 1. On the other hand, for LUT ε'', *sensor-A* is more sensitive than *sensor-B*, with sensitivities $\Delta Q/\Delta\varepsilon''$ of 70.17/$\Delta\varepsilon''$ and 55.87/$\Delta\varepsilon''$, respectively; $\Delta\varepsilon''$ is increment in LUT ε'' of 1.

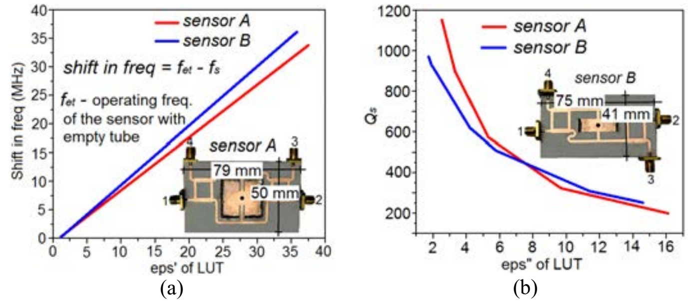

Fig. 4. (a) Sensitivity of LUT ε' and photograph of *sensor-A*, (b) sensitivity of LUT ε'' and photograph of *sensor-B*.

The maximum operating frequency shift of both sensors lies within a bandwidth of 1%. Maximum deviation with the standard samples [8] from the LUT characterization with *sensor-A* are 1.1% for ε' and 54.7% for ε''; while those using *sensor-B* are 10.3% and 18% for ε' and ε'', respectively.

V. CONCLUSION

Two planar circuits for chipless RFID tags for sensing complex-dielectric permittivity of liquids were presented. The first sensor (*sensor-A*) is based on an SIW cavity resonator while the second (*sensor-B*) makes use of an SIW ENZ tunnel structure. Several liquids were successfully measured and characterized using the Cavity-Perturbation-Technique for SIW circuits.

REFERENCES

[1] L. F. Chen, C. K. Ong, C. P. Neo, V. V. Varadan, V. K. Varadan, *Microwave Electronics, Measurement and Materials Characterization*, John Wiley & Sons, 2004.

[2] K. Saeed, R. D. Pollard, I. C. Hunter, "Substrate Integrated Waveguide Cavity Resonators for Complex Permittivity Characterization of Materials", *IEEE Trans. Microwave Theory & Tech.,* vol. 56, no. 10, pp. 2340-2347, Oct. 2008.

[3] H. Lobato-Morales, D.V.B. Murthy, A. Corona-Chavez, J. L. Olvera-Cervantes, J. Martinez-Brito, L. G. Guerrero-Ojeda, "Permittivity Measurements at Microwave Frequencies using Epsilon-Near-Zero (ENZ) Tunnel Structure", *IEEE Trans. Microwave Theory & Tech.* vol. 59, no. 7, pp. 1863-1868, Jul. 2011.

[4] S. Preradovic, N., M. Kamakar, E. M. Amin, "Chipless RFID Tag with Integrated Resistive and Capacitive Sensors", *2011 Asia-Pacific Microwave Conf. Proc.* pp. 1354-1357, Dec. 2011.

[5] D. M. Pozar, *Microwave Engineering*, 3rd ed. New York, Wiley: 2005.

[6] Sonnet Software, Full-wave EM circuit simulator, v. 13.

[7] Ansoft HFSS, Full-wave EM structure simulator, v. 13.

[8] A. P. Gregory, R. N. Clarke, "Tables of the complex permittivity of dielectric reference liquids up to 5 GHz", *Nat. Phys. Lab. Report*, CETM 33, U.K., Jan. 2012.

978-1-4673-2141-9/13/$31.00 ©2013 IEEE